Oligomerization of the α_{1a}- and α_{1b}-Adrenergic Receptor Subtypes

POTENTIAL IMPLICATIONS IN RECEPTOR INTERNALIZATION*

Laura Stanasila‡§, Jean-Baptiste Perez§¶, Horst Vogel¶‖, and Susanna Cotecchia‡

From the ‡Institut de Pharmacologie et de Toxicologie, Université de Lausanne, 1005 Lausanne and ¶Laboratoire de Chimie Physique des Polymères et Membranes, Ecole Polytechnique Fédérale de Lausanne, 1015 Ecublens, Switzerland

We combined biophysical, biochemical, and pharmacological approaches to investigate the ability of the α_{1a}- and α_{1b}-adrenergic receptor (AR) subtypes to form homo- and hetero-oligomers. Receptors tagged with different epitopes (hemagglutinin and Myc) or fluorescent proteins (cyan and green fluorescent proteins) were transiently expressed in HEK-293 cells either individually or in different combinations. Fluorescence resonance energy transfer measurements provided evidence that both the α_{1a}- and α_{1b}-AR can form homo-oligomers with similar transfer efficiency of ~0.10. Hetero-oligomers could also be observed between the α_{1b}- and the α_{1a}-AR subtypes but not between the α_{1b}-AR and the β_2-AR, the NK1 tachykinin, or the CCR5 chemokine receptors. Oligomerization of the α_{1b}-AR did not require the integrity of its C-tail, of two glycophorin motifs, or of the N-linked glycosylation sites at its N terminus. In contrast, helix I and, to a lesser extent, helix VII were found to play a role in the α_{1b}-AR homo-oligomerization. Receptor oligomerization was not influenced by the agonist epinephrine or by the inverse agonist prazosin. A constitutively active (A293E) as well as a signaling-deficient (R143E) mutant displayed oligomerization features similar to those of the wild type α_{1b}-AR. Confocal imaging revealed that oligomerization of the α_1-AR subtypes correlated with their ability to co-internalize upon exposure to the agonist. The α_{1a}-selective agonist oxymetazoline induced the co-internalization of the α_{1a}- and α_{1b}-AR, whereas the α_{1b}-AR could not co-internalize with the NK1 tachykinin or CCR5 chemokine receptors. Oligomerization might therefore represent an additional mechanism regulating the physiological responses mediated by the α_{1a}- and α_{1b}-AR subtypes.

G protein-coupled receptors (GPCR),[1] known also as heptahelical receptors, form the largest family of transmembrane signaling proteins transducing signals arising from ions, hormones, neurotransmitters, odorants, chemoattractants, and photons. GPCRs were for a long time presumed to function as monomers according to the prevailing model: one ligand molecule-one receptor-one G protein. Recently, increasing complexity of GPCR function and regulation has progressively emerged. For example, one GPCR can adopt multiple conformational states able to interact differentially with signaling and regulatory proteins (1, 2). In addition, receptor cross-talks both at the G protein and at downstream signaling levels have often been described (3, 4). Recently, it was shown that cross-talk among GPCRs can also occur at the receptor level by means of receptor oligomerization (reviewed in Refs. 5–7). One of the early indications suggesting the capacity of GPCRs to oligomerize came from pharmacological studies showing positive or negative cooperativity of ligand binding curves. More recent support was provided by some "complementation" studies in which co-expression of two GPCR mutants could rescue their functional defects (8). These results were interpreted as evidence of inter-molecular interactions between two receptor mutants according to a "domain swapping" model (9). Further indication of GPCR oligomerization came from a large number of studies using co-immunoprecipitation of epitope-tagged receptors co-expressed in the same cells or fluorescence spectroscopy to monitor such oligomers in live cells (reviewed in Refs. 5–7).

The molecular basis of GPCR oligomerization is not yet fully understood. Co-immunoprecipitation relies on receptor solubilization, which can result in artifactual aggregation of the proteins. To overcome these limits fluorescence spectroscopy techniques, like fluorescence or bioluminescence resonance energy transfer, have been increasingly used. It is widely accepted that energy transfer measurements are well suited to monitor protein-protein interactions or proximity in live cells, as FRET only occurs when the distance between the two fluorophores falls below ~100 Å (10). So far, in virtually all studies an increased energy transfer signal between GPCRs has been interpreted as the evidence for receptor oligomerization. However, whether receptor oligomerization involves intramolecular interactions among receptors *versus* their increased proximity within the cell membrane without direct contact cannot be unequivocally demonstrated either by the energy transfer measurements or by the results of co-immunoprecipitation experiments. Therefore, in this study the term receptor "oligomerization" will be used bearing in mind that the precise molecular events underlying this phenomenon are not fully understood.

[1] The abbreviations used are: GPCR, G protein-coupled receptor; AR, adrenergic receptor(s); G protein, guanylyl nucleotide binding regulatory protein; IP, inositol phosphate; DMEM, Dulbecco's modified Eagle's medium; FRET, fluorescence resonance energy transfer; [^{125}I]HEAT, [^{125}I]iodo-2-[β-(4-hydroxyphenyl)-ethylaminomethyl]tetralone; CFP, cyan fluorescent protein; GFP, green fluorescent proteins; HA, hemagglutinin; GABA$_B$, γ-aminobutyric acid, type B; RANTES, regulated on activation normal T cell expressed and secreted; FITC, fluorescein isothiocyanate; PBS, phosphate-buffered saline; ER, endoplasmic reticulum; YFP, yellow fluorescent protein.

The functional implication of the existence of GPCR homo- and hetero-oligomers has been addressed by several studies. The strongest evidence supporting the functional importance of hetero-oligomerization came from studies on the metabotropic GABA$_B$ receptor. The full reconstitution of the functional activity of the GABA$_B$ receptor requires the oligomerization between the GABA$_B$-R1 and GABA$_B$-R2 receptor monomers (11). For other GPCRs, a role of oligomerization in receptor signaling as well as internalization has been suggested (reviewed in Refs. 5–7). However, much work is still required to elucidate how oligomerization is involved in these distinct processes. In addition, whereas the majority of studies was performed in recombinant systems, only in a few cases was evidence provided that GPCR oligomerization occurs in physiological systems. For example, in a recent study hetero-oligomers formed by the adenosine A1 and glutamate mGluR1 receptors were isolated from cerebellar neuronal cultures (12). In addition, hetero-oligomers formed by the angiotensin II AT1 and bradykinin B2 receptors were isolated in platelets of pre-eclamptic pregnant women (13).

Within the adrenergic receptor (AR) family, oligomerization has been extensively studied for the β_2-AR (14–16), and these studies have often represented an important reference for investigating the oligomerization of other GPCRs. The β_2-AR can form both homo- and hetero-oligomers with the δ- and κ-opioid receptors (17) as well as with the β_1-AR (18). Homo-oligomerization of the β_2-AR is constitutive, but it can also be enhanced by exposure to the agonist (16). In contrast to the amount of information available for the β_2-AR and several other GPCRs, nothing is known so far on the putative oligomeric state of the α_1-AR subtypes.

In this study we extensively investigated the ability of the α_{1a}- and α_{1b}-AR subtypes to oligomerize using biophysical, biochemical, as well as pharmacological approaches. FRET measurements provided solid evidence that both recombinant α_{1a}- and α_{1b}-AR subtypes can selectively form homo- and hetero-oligomers. Our results suggest that the homo-oligomerization of the α_{1b}-AR involves the participation of helix I and, to a lesser extent, of helix VII. The results of confocal imaging strongly suggest that receptor oligomerization plays a role in receptor endocytosis, which might have implications for the physiological responses mediated by the α_{1a}- and α_{1b}-AR subtypes.

EXPERIMENTAL PROCEDURES

Materials—The plasmid encoding the chemokine CCR5 receptor and RANTES were kind gifts of Dr. Jean-Luc Galzi, UPR 9050 CNRS, Illkirch, France. The NK1-pEGFP-N1 plasmid was a kind gift of Dr. Bruno Meyer, EPFL, Lausanne, Switzerland. The pEGFP-N1, pECFP-N1, and pEYFP-N1 vectors were from Clontech. Immobilon membranes were from Millipore. Prolong mounting medium was from Molecular Probes. Monoclonal anti-c-Myc antibodies, protein A-Sepharose, epinephrine, and prazosin from Sigma. *Pwo* DNA polymerase, complete protease inhibitor mixture, and restriction enzymes were from Roche Applied Science. Monoclonal and polyclonal anti-HA antibodies were from Santa Cruz Biotechnology. Fluorescein- and rhodamine-coupled anti-rabbit and rhodamine-coupled anti-mouse antibodies were from The Jackson Laboratories. Anti-rabbit and anti-mouse horseradish peroxidase-coupled antibodies, [125I]iodocyanopindolol, and ECL Western blotting detection reagent were from Amersham Biosciences. Protein assay (Bradford) was from Bio-Rad. Effectene transfection reagent was from Qiagen. DMEM, fetal calf serum, fungizone, and gentamycin were from Invitrogen. [125I]HEAT and [3H]inositol were from PerkinElmer Life Sciences.

Construction of Receptor-GFP and CFP Fusion Proteins and Site-directed Mutagenesis—The full-length cDNA encoding the hamster α_{1b}-AR (19) was PCR-amplified and inserted into the pEGFP-N1 and pECFP-N1 vectors using *EcoRI/AgeI* to give the α_{1b}-pEGFP-N1 and α_{1b}-pECFP-N1 vectors, respectively. The cDNA encoding the α_{1b}-AR fused to GFP (α_{1b}-GFP) was also subcloned in the pRK5 using *EcoRI/XbaI* to give the α_{1b}-GFP-pRK5 vector. The Thr³⁶⁹-GFP, Thr³⁶⁹-CFP,

and Thr³⁶⁹-YFP constructs were obtained by PCR-amplifying a DNA fragment of the α_{1b}, encompassing amino acids 1–369 and subcloning it at the *EcoRI-AgeI* sites into the α_{1b}-GFP-pRK5, α_{1b}-pECFP-N1, and pEYFP-N1 vectors, respectively. The R143E-GFP and A293E-GFP constructs were obtained by replacing the *EcoRI-BssHII* fragment of the previously described R143E and A293E mutants (20, 21) into the α_{1b}-GFP-pRK5 vector. The G53L and G301L mutants were constructed by PCR mutagenesis and subcloned into the α_{1b}-GFP-pRK5 vector to give the G53L-GFP and G301L-GFP constructs, respectively. The construction of the N-glycosylation-deficient mutant N4 fused to GFP (N4-GFP) was described previously (22).

Fragments of the α_{1b}-AR lacking different transmembrane helices were constructed by PCR introducing *EcoRI* and *BssHII* sites at their 5' and 3' ends, respectively, and subcloned into the Thr³⁶⁹-YFP at the *EcoRI* site (which is in the 5'-untranslated) and *BssHII* site (corresponding to amino acids 356 and 357). The receptor fragments engineered were the following: α1b(I–III), amino acids 1–148; α1b(I–V), amino acids 1–231; α1b(III–VII), amino acids 112–369; and α1b(V–VII), amino acids 195–369. All the fragments included 4–5 residues beyond the helical portion as well as also amino acids 356–369 of the C-tail before the fluorophore.

The α_{1b}/β_2 adrenergic chimeric receptors were constructed using PCR by replacing each helix of the hamster α_{1b}-AR with the corresponding segment of the human β_2-AR. The helices were defined based on sequence alignment and on the x-ray structure of rhodopsin. The residues of the α_{1b}-AR replaced with those of the β_2-AR for each helix (h) were the following: hI (Ala⁴⁵–Ala⁷¹ α_{1b}/Val³³–Ala⁵⁹ β_2); hII (Thr⁸⁰–Val¹⁰⁷ α_{1b}/Thr⁶⁸–Leu⁹⁵ β_2); hIII (Phe¹¹⁷–Tyr¹⁴⁴ α_{1b}/Trp¹⁰⁵–Tyr¹³³ β_2); hIV (Ala¹⁶²–Leu¹⁸¹ α_{1b}/Ala¹⁵⁰–Ile¹⁶⁹ β_2); hV (Tyr²⁰³–Val²²⁶ α_{1b}/Tyr¹⁹⁹–Val²²² β_2); hVI (Arg²⁸⁸–Leu³¹⁶ α_{1b}/Lys²⁶⁷–Val²⁹⁵ β_2); hVII (Val³²⁹–Ile³⁶² α_{1b}/Val³⁰⁷–Leu³⁴⁰ β_2). The percentage of sequence identity between the portions replaced in each helix was 38% for hI, 50% for hII, 57% for hIII, 30% for hIV, 50% for hV, 65% for hVI, and 41% for hVII.

The full-length cDNA encoding the human α_{1a}-AR (23) was PCR-amplified and inserted into the pEGFP-N1 and pECFP-N1 vectors using *EcoRI/AgeI* (blunted) to give the α_{1a}-GFP and α_{1a}-CFP constructs, respectively. The full-length cDNA encoding the human β_2-AR was PCR-amplified and subcloned into the pEGFP-N1 using *HindIII/AgeI* to give the β_2-GFP construct. The full-length cDNA encoding the chemokine CCR5 receptor was PCR-amplified and subcloned into the pECFP-N1 using *HindIII/AgeI* to give the CCR5-CFP construct.

Construction of Epitope-tagged Receptors—The C-terminal fragments of the α_{1a}-AR and the α_{1b}-AR were amplified using primers encoding the HA (YPYDVPDYA) or Myc (EQKLISEEDL) epitopes at the 3' end and inserted into the α_{1b}-AR-pRK5 (using *BamHI/HindIII*) or α_{1a}-AR-pRK5 (using *EcoRV/BamHI*) vectors, respectively. The full-length cDNA encoding the chemokine CCR5 receptor was PCR-amplified using a primer encoding the Myc epitope at the 5' end and subcloned into the pRK5 vector using *BamHI/HindIII*. The full-length cDNA encoding the tachykinin NK1 receptor was amplified using a primer encoding the Myc epitope at the 3' end and subcloned into the pRK5 vector using *EcoRV/HindIII*.

Cell Culture and Transfection—HEK-293 cells were grown in DMEM supplemented with 10% fetal calf serum and gentamycin (100 μg/ml) (37 °C and 5% CO$_2$) and transfected using the calcium-phosphate method or the transfection reagent Effectene following the manufacturer's protocol. For inositol phosphate determination, cells (0.15 × 10⁶) were seeded in 12-well plates and transfected with 0.2–0.5 μg/well using Effectene. For ligand binding, FRET, and immunoprecipitation experiments, cells were grown in 100-mm dishes and transfected with a maximum of 20 μg of DNA/dish using the calcium-phosphate method. For confocal imaging cells were grown on glass coverslips in 6-well dishes and transfected with 1–2 μg of DNA/well using the calcium-phosphate method. For cells transfected with different combinations of plasmids, the total amount of transfected DNA was kept constant in the samples using pRK5.

Membrane Preparation and Ligand Binding—48 h after transfection, cells were washed in PBS, scraped off the culture plates, and collected in ice-cold membrane buffer (5 mM Tris, 0.5 mM EDTA, pH 7.4). After centrifugation at 40,000 × g, the pellet was resuspended in ice-cold membrane buffer and Polytron-homogenized. Protein concentration was determined using the Bradford protein assay. For ligand binding of [125I]HEAT, the membranes were resuspended in binding buffer (50 mM Tris, 0.5 mM EDTA, 150 mM NaCl, pH 7.4) and incubated with the radioligand for 1 h at 25 °C. [125I]HEAT was used at a concentration of 250 pM for measuring receptor expression at a single concentration and of 80 pM for competition binding analysis. For saturation binding experiments, the radioligand concentration ranged between 10

and 400 pM. Prazosin at 10^{-6} M was used to determine nonspecific binding. Saturation analysis and competition curves were analyzed using Prism 3.02 (GraphPad Software Inc., San Diego).

Inositol Phosphate Accumulation—24–36 h after transfection, cells were labeled for 12 h with myo-[^{3}H]inositol at 4 μCi/ml in inositol-free DMEM supplemented with 1% fetal bovine serum. Cells were pre-incubated for 10 min in PBS containing 20 mM LiCl and then stimulated for 45 min with different concentrations of epinephrine. Total inositol phosphates were extracted and separated as described previously (19).

SDS-PAGE and Western Blotting—Samples were denatured in SDS-PAGE loading buffer (65 mM Tris, 2% SDS, 5% glycerol, 5% β-mercaptoethanol, pH 6.8) for 1 h at room temperature, separated on 10% acrylamide gels, and electroblotted onto Immobilon membranes. Blots were incubated in TBS buffer (50 mM Tris, 150 mM NaCl, pH 8) containing 0.05% Tween 20, 5% (w/v) powder milk, and the primary antibody (mouse monoclonal anti-HA or anti-Myc) diluted 1:200. After the primary antibody was washed, the secondary anti-mouse antibody linked to horse-radish peroxidase was added, and the blots were developed using the enhanced chemiluminescence (ECL) detection system.

Immunoprecipitation of Receptors—36 h after transfection, cells were washed twice with PBS and scraped off the culture plates in ice-cold buffer containing 5 mM Tris and 5 mM EDTA, pH 7.4. After centrifugation at 40,000 $\times$ g, the pellet was resuspended in 1 ml of ice-cold lysis buffer (20 mM Tris, 0.5 mM EDTA, 1% digitonin, 100 mM NaCl, pH 7.4) containing a complete protease inhibitor mixture. Solubilization was carried out for 3 h at 4 °C on a spinning wheel. Unsolubilized material was pelleted by centrifugation for 15 min at 20,000 $\times$ g on a bench-top centrifuge. The supernatant was incubated with 5 μg of anti-HA polyclonal antibody overnight on the spinning wheel at 4 °C. After addition of 2.5% (w/v) protein A-Sepharose, the incubation was continued for 2 h at 4 °C, followed by a brief centrifugation on a bench-top centrifuge. The pellet was washed three times in the lysis buffer, once in PBS, and then dissolved in SDS-PAGE loading buffer for 1 h at 37 °C.

Fluorescence Spectroscopy—48 h after transfection, cells were washed in PBS and detached from the plates using PBS containing 0.5 mM EDTA. The cells from one 10-cm culture dish were resuspended in 1 ml of isotonic buffer (137.5 mM NaCl, 1.25 mM MgCl$_2$, 1.25 mM CaCl$_2$, 6 mM KCl, 5.6 mM glucose, 10 mM HEPES, 0.4 mM NaH$_2$PO$_4$, pH 7.4) and used in spectrofluorimetric measurements. Cells were routinely co-transfected with equal amounts of plasmids encoding the receptors fused to GFP or to CFP (5–10 μg of each plasmid/100-mm diameter dish) in order to approach a CFP:GFP ratio of 1.

Fluorescence spectra of cell suspensions were recorded on a SPEX Fluorolog II (Instruments S.A., Stanmore, UK). Samples were placed in a 10 $\times$ 4-mm^2 quartz cuvette (Hellma, Germany) and continuously stirred by a magnetic stirrer. Excitation and emission slits were set at 2-nm band path. CFP and GFP were excited at 430 and 488 nm, respectively, and their fluorescence measured at 450–540 and 500–540 nm, respectively.

The spectral contributions arising from light scattering and nonspecific fluorescence of the cells were eliminated by subtracting the emission spectra of mock-transfected cells from the fluorescence spectra of cells expressing the receptor-CFP and GFP constructs. To do so, we measured the emission intensity at 450 nm upon excitation at 430 nm, considering that CFP or GFP fluorescence is negligible and that only light scattering contributes to emission at this wavelength. We then calculated the ratio between the intensities at 450 nm in mock-transfected *versus* cells expressing the fluorescent receptors and used it as a correction factor F(background). The spectrum of the mock-transfected cells divided by the F(background) was then subtracted from the spectrum of the cells expressing receptor-CFP and GFP constructs.

To take into account the differences in expression level of the receptor-CFP and -GFP constructs in co-transfected cells, a second normalization step was adopted. The fluorescence spectra of cells individually expressing the receptor-CFP and -GFP constructs were measured and divided by a correction factor F. For the receptor-CFP excited at 430 nm: F(CFP) = CFP(430/465)/CFP and GFP(430/465). For the receptor-GFP excited at 430 nm: F(GFP) = GFP(490/510)/CFP and GFP(490/510).

After normalizing for cell density, FRET was measured by subtracting from the emission spectrum of cells expressing both fluorescent receptors the emission spectra obtained by excitation at 430 nm of cells individually expressing the receptor-CFP and GFP constructs, each divided by its respective correction factor F. The resulting spectrum in cells expressing both fluorescent receptors corresponds to GFP emission arising exclusively from FRET. The transfer efficiency E was determined as shown in Equations 1 and 2,

$$E = \frac{A_A(\lambda_D)}{A_D(\lambda_D)}\left(\frac{I_{AD}(\lambda_D,\lambda_{A(\text{emi})})}{I_A(\lambda_D,\lambda_{A(\text{emi})})} - 1\right) \quad \text{(Eq. 1)}$$

where

$$\frac{A_A(\lambda_D)}{A_D(\lambda_D)} = \frac{\epsilon_A(\lambda_D)}{\epsilon_D(\lambda_D)} \cdot \frac{I_A(\lambda_A,\lambda_{A(\text{emi})}) \cdot \epsilon_D(\lambda_D)\phi_D(\lambda_{D(\text{emi})})}{\frac{I_{DA}(\lambda_D,\lambda_{D(\text{emi})})}{1-E} \cdot \epsilon_A(\lambda_A)\phi_A(\lambda_{A(\text{emi})})} \quad \text{(Eq. 2)}$$

and λ_D, 430 nm; λ_A, 490 nm; $\lambda_{D(\text{emi})}$, 475 nm; $\lambda_{A(\text{emi})}$, 510 nm; absorption coefficient of the donor at λ_D, $\epsilon_A(\lambda_D) = 13,750$ cm^{-1} M^{-1}; absorption coefficient of the acceptor at λ_A, $\epsilon_A(\lambda_A) = 55,000$ cm^{-1} M^{-1}; fluorescence quantum yield of the donor, $\phi_D = 0.4$; fluorescence quantum yield of the acceptor, $\phi_A = 0.6$; $A_A(\lambda_D)$, acceptor absorbance at the wavelength of donor excitation; $A_D(\lambda_D)$, donor absorbance at the wavelength of donor excitation; $I_A(\lambda_D, \lambda_{A(\text{emi})})$, fluorescence intensity of the acceptor at $\lambda_{A(\text{emi})}$ when excited at λ_D; $I_{AD}(\lambda_D, \lambda_{A(\text{emi})})$, fluorescence intensity of the acceptor at $\lambda_{A(\text{emi})}$ when excited at λ_D in the presence of the donor; $I_{DA}(\lambda_D, \lambda_{D\text{em}})$, fluorescence intensity of the donor at $\lambda_{D(\text{emi})}$ when excited at λ_D in the presence of the acceptor.

The GFP:CFP ratio was given by Equation 3,

$$\frac{C_A}{C_D} = \frac{I_A(\lambda_A,\lambda_{A(\text{emi})}) \cdot \epsilon_D(\lambda_D)\phi_D(\lambda_{D(\text{emi})})}{\frac{I_{DA}(\lambda_D,\lambda_{D(\text{emi})})}{1-E} \cdot \epsilon_A(\lambda_A)\phi_A(\lambda_{A(\text{emi})})} \quad \text{(Eq. 3)}$$

where C_D is the concentration of the donor (CFP); C_A is the concentration of the acceptor (GFP).

For FRET measurements on receptor fragments fused to YFP, the elaboration of the results described above was adapted to fit the YFP properties. CFP and YFP were excited at 430 and 500 nm, respectively, and their fluorescence was measured at 450–570 and 520–570 nm, respectively. In this case, the acceptor parameters used are as follows: λ_A, 500 nm; $\lambda_{A(\text{emi})}$, 530 nm; quantum yield of acceptor ϕ_A, 0.6; $\epsilon_A(\lambda_D)$, 3530 cm^{-1} M^{-1}; $\epsilon_A(\lambda_A) = 43,700$ cm^{-1} M^{-1}.

To determine the effect of ligands on FRET efficiency, cell suspensions were incubated at saturating concentrations of epinephrine (10^{-4} M) or prazosin (10^{-6} M) for 15 min at 37 °C under gentle shaking. Spectra of treated and untreated cells were recorded at 37 °C.

Internalization Experiments—36 h after transfection, cells grown on glass coverslips were treated for 1 h with vehicle or with a saturating concentration of different agonists (10^{-4} M epinephrine, 10^{-5} M oxymetazoline, 10^{-4} M substance P, or 10^{-6} M RANTES). After treatment, cells were washed with PBS, fixed with formaldehyde, and permeabilized for 5 min in 0.2% Triton. For immunostaining of cells expressing the HA-tagged receptors, the cells were incubated for 1 h in PBS containing 1% BSA and for another hour in PBS containing 0.1% BSA, and the polyclonal anti-HA antibody was diluted at 1:100. After a second incubation with the anti-rabbit rhodamine-coupled antibody diluted at 1:100 in PBS containing 0.1% BSA, the coverslips were washed three times in PBS and mounted in Prolong mounting medium. For immunostaining of cells co-expressing the α_{1b}-HA and myc-CCR5, the polyclonal anti-HA and the monoclonal anti-Myc antibodies were used, followed by the anti-rabbit FITC-coupled and the anti-mouse rhodamine-coupled secondary antibodies. Cells immunostained with fluorescent antibodies were analyzed by confocal imaging.

Confocal Imaging—Cells expressing different fluorescent receptors were imaged using a Zeiss LSM510 confocal microscope equipped with a C-apochromat $\times$63/1.2-watt water immersion objective (Zeiss, Germany). The following laser lines were used for excitation: 458 nm for CFP, 488 nm for GFP and FITC, and 543 nm for rhodamine. The following Zeiss filter sets were used to detect the fluorescence of a particular fluorophore: LP475 for CFP, BP505–550 for GFP and FITC, and LP543 for rhodamine. The pinhole was kept at ~1 airy unit for all recordings.

RESULTS

Functional Characterization of the Tagged Receptors—To investigate the pharmacological properties of the α_1-AR subtypes tagged with different epitopes (HA and Myc) or fluorescent proteins (GFP and CFP), the receptors were expressed in HEK-293 cells and tested for their ability to bind the radioligand [^{125}I]HEAT and epinephrine. Saturation binding experiments indicated that the K_D values of [^{125}I]HEAT were similar at the various tagged or non-tagged α_1-AR constructs (results not shown). As shown in Table I, the expression levels of the

TABLE I

Pharmacological properties of different $\alpha 1$-AR constructs

[^{125}I]HEAT binding was measured on membranes prepared from HEK-293 cells expressing the wild type $\alpha 1a$ and $\alpha 1b$-AR or their constructs tagged with different epitopes (HA or Myc) or fluorescent proteins (CFP or GFP). Expression was measured using 250 pM [^{125}I]HEAT on membranes from 1 well of a 6-well dish (200 μg of proteins/well). The inositol phosphate (IP) accumulation in the absence (basal) or presence of 10^{-4} M epinephrine (Epi-stimulated) is expressed as % of the levels measured in mock-transfected cells. Results are the mean ± S.E. of at least three independent experiments performed in triplicate. The other receptor-CFP fusion constructs used in this study behaved like their wild type counterparts (results not shown).

Receptor	Expression	Basal IP	Epi-stimulated IP	IC$_{50}$ Epi
	fmol/well	*%*		*μM*
wt $\alpha 1b$	961 ± 100	104 ± 13	898 ± 28	5.31 ± 0.36
$\alpha 1b$-GFP	989 ± 354	105 ± 7	794 ± 82	5.73 ± 1.3
$\alpha 1b$-CFP	1055 ± 102	102 ± 12	809 ± 40	22.37 ± 4.7
T369-GFP	892 ± 341	122 ± 2	1068 ± 107	4.14 ± 0.7
A293E-GFP	382 ± 188	1478 ± 144[a]	1923 ± 55[a]	0.12 ± 0.02[a]
R143E-GFP	511 ± 107	133 ± 18	125 ± 16[a]	0.04 ± 0.01[a]
G53L-GFP	875 ± 55	112 ± 5	492 ± 99[a]	1.76 ± 0.1
G301L-GFP	665 ± 103	118 ± 6	321 ± 41[a]	2.23 ± 0.3
$\alpha 1b$-HA	653 ± 127	181 ± 21	1068 ± 87	5.92 ± 1.7
$\alpha 1b$-myc	556 ± 21	150 ± 29	1181 ± 170	5.38 ± 2.7
wt $\alpha 1a$	658 ± 116	148 ± 29	1953 ± 90	6.87 ± 0.4
$\alpha 1a$-GFP	253 ± 111	161 ± 20	2260 ± 287	10.72 ± 3.3
$\alpha 1a$-HA	508 ± 24	126 ± 8	1223 ± 318	8.51 ± 0.3
$\alpha 1a$-myc	656 ± 180	133 ± 3	1947 ± 186	8.27 ± 0.9

[a] Paired Student's t test, $p < 0.05$ compared with wt $\alpha 1b$.

various receptors ranged between 300 and 900 fmol/well. The IC$_{50}$ values of epinephrine were similar at the tagged or non-tagged wild type α_{1a}- and α_{1b}-AR subtypes (Table I). The affinity for epinephrine of the α_{1b}-AR mutants A293E, R143E, and truncated Thr^{369} fused with GFP (A293E-GFP, R143E-GFP, and Thr^{369}-GFP) was comparable with that previously reported for the non-tagged receptor mutants (21, 20, 24). Coupling of the different α_1-AR constructs to the G$_q$/phospholipase C pathway was assessed as their ability to mediate epinephrine stimulated IP accumulation (Table I). The IP accumulation mediated by the α_{1b}-AR or α_{1a}-AR differently tagged was overall similar to that of the wild type receptor. The A293E-GFP was constitutively active, whereas the R143E-GFP was signaling-deficient as reported previously (20, 21) for the non-tagged mutants A293E and R143E. The ability of the Thr^{369}-GFP receptor to mediate IP accumulation was similar to that of the wild type α_{1b}-AR as reported previously for the non-tagged truncated mutants (24). In contrast, both the G53L-GFP and G301L-GFP carrying mutations of the glycophorin motifs in helix 2 and 6, respectively, were impaired in their signaling ability despite having normal ligand binding properties. The NK1-GFP receptor was functional as demonstrated by its ability to mediate IP accumulation (results not shown) and to internalize in response to substance P (Fig. 9). For the β_2-AR and CCR5 chemokine receptors, previous studies (16) have reported that fusion to derivatives of GFP did not significantly change their functional features.

To assess whether the fluorescent receptor constructs were properly localized at the plasma membrane, we used confocal imaging of fixed HEK-293 cells transiently expressing the different receptors fused to GFP or CFP. As shown in Fig. 1, all the fluorescent receptor constructs listed in Table I were expressed at the cell surface as indicated by the sharp fluorescence at the plasma membrane. The fluorescent receptor constructs also displayed some intracellular fluorescence which was however more pronounced for the A293E-GFP (Fig. 1g). This is consistent with previous findings suggesting that the constitutively active A293E mutant is also constitutively internalized (21).

Homo-oligomerization of the α_{1b}-AR—To explore whether the α_{1b}-AR can oligomerize, the α_{1b}-CFP and α_{1b}-GFP were co-expressed in HEK-293 cells, and FRET was measured on cell suspensions (as described under "Experimental Procedures"). This fluorophore couple fulfils the conditions necessary for

FRET to occur because the fluorescence spectrum of CFP (acting as a donor) largely overlaps with the excitation spectrum of GFP (acting as acceptor).

In preliminary experiments, we established that transfection of cells with equal amounts of DNA encoding the α_{1b}-CFP or α_{1b}-GFP resulted in a GFP:CFP expression ratio ranging from 0.8 to 1.3 (results not shown). Because the radioligand [^{125}I]HEAT could not discriminate between the two fluorescent constructs, we determined the relationship of fluorescence intensity *versus* receptor expression measured by radioligand binding for the α_{1b}-CFP and α_{1b}-GFP expressed individually (results not shown). Based on the results of these calibration curves, we assessed that in the FRET experiments the amount of the α_{1b}-CFP and α_{1b}-GFP co-expressed in each sample was about 1–2 pmol/mg of protein for each construct.

Fig. 2A shows the results from a representative FRET experiment in HEK-293 cells co-expressing the α_{1b}-CFP and α_{1b}-GFP. Spectra were recorded from mock-transfected cells and from cells expressing either the donor (α_{1b}-CFP; *indigo trace*), the acceptor (α_{1b}-GFP; *green trace*), or both (*blue trace*). After subtracting the light scattering and nonspecific fluorescence as well as normalizing for the expression of the individual fluorescent receptor constructs (as described under "Experimental Procedures"), a typical GFP fluorescence spectrum (*red trace*) became apparent suggesting that energy transfer had occurred between the α_{1b}-CFP and α_{1b}-GFP. The approach we adopted was similar to that used to monitor the oligomerization of the Ste2 pheromone receptor in yeast cells (25).

Two types of control experiments were performed to prove that the GFP fluorescence spectrum resulted from FRET between the two receptor constructs co-expressed in the same cell. In the first experiment, two cell populations were mixed, one expressing only the α_{1b}-CFP and the other only the α_{1b}-GFP. In the mixed cell population FRET was not observed, indicating that it is the result of the donor-acceptor interaction, occurring only when the fluorescent receptors are co-expressed in the same cells (Fig. 2B). In the second experiment, the wild type α_{1b}-AR was co-expressed with the α_{1b}-CFP and α_{1b}-GFP. In these cells, the FRET signal was significantly decreased (Fig. 2C) likely because the non-fluorescent α_{1b}-AR could competitively inhibit the donor-acceptor interaction. These findings lead us to conclude that the α_{1b}-ARs do form homo-oligomers within the cell.

The energy transfer efficiency between α_{1b}-CFP and α_{1b}-GFP

FIG. 1. **Expression of fluorescent receptor constructs.** Confocal images were taken of fixed HEK-293 cells expressing different fluorescent receptor constructs. *a*, α_{1b}-GFP; *b*, Thr^{369}-GFP; *c*, α_{1a}-GFP; *d*, β_2-GFP; *e*, NK1-GFP; *f*, CCR5-CFP; *g*, A293E-GFP; *h*, R143E-GFP; *i*, G53L-CFP; *j*, G301L-GFP; *k*, N4-CFP.
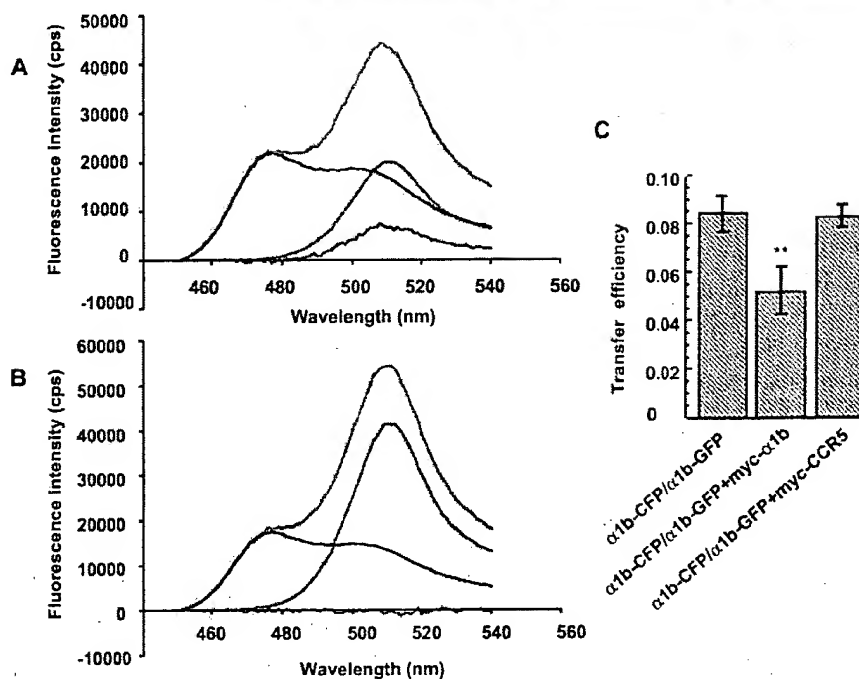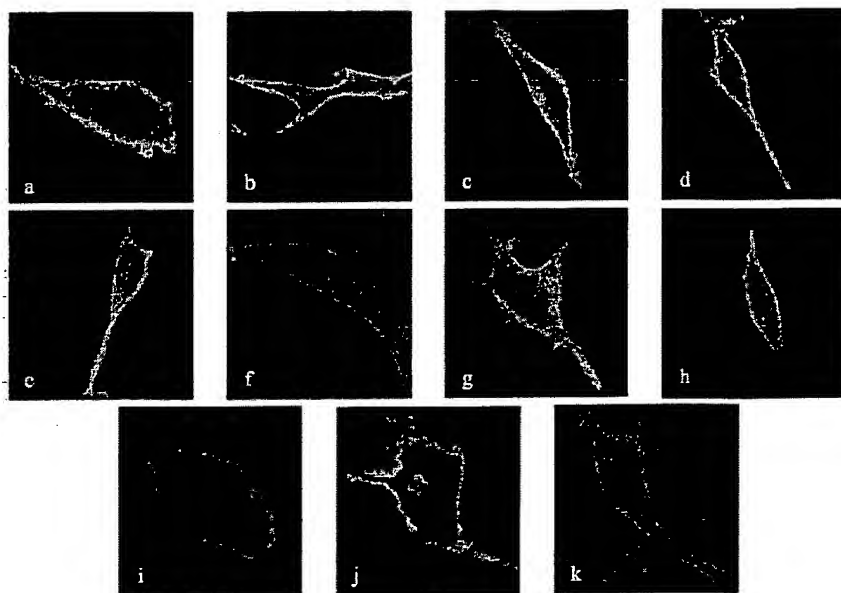
FIG. 2. **FRET measurements.** HEK-293 cells expressing the α_{1b}-CFP and α_{1b}-GFP individually or in combination were excited at 430 nm, and emission spectra were recorded. *A*, *blue*, spectrum from cells co-expressing the α_{1b}-CFP and α_{1b}-GFP; *indigo*, spectrum from cells expressing the α_{1b}-CFP (normalized as indicated under "Experimental Procedures"); *green*, spectrum from cells expressing the α_{1b}-GFP (normalized as indicated under "Experimental Procedures"); *red*, FRET obtained by subtracting the green and indigo spectra from the blue emission spectrum. *B*, *blue*, spectrum from a 1:1 mixture of cells individually expressing the α_{1b}-CFP and α_{1b}-GFP; *indigo*, spectrum from cells expressing the α_{1b}-CFP (normalized as indicated under "Experimental Procedures"); *green*, spectrum from cells expressing the α_{1b}-GFP (normalized as indicated under "Experimental Procedures"); *red*, FRET obtained by subtracting the green and indigo spectra from the blue emission spectrum. *C*, FRET efficiency in cells co-expressing the α_{1b}-CFP and α_{1b}-GFP in the absence (α_{1b}-CFP/α_{1b}-GFP) or in the presence of the wild type α_{1b}-AR (α_{1b}-CFP/α_{1b}-GFP + α1b) or myc-CCR5 (α_{1b}-CFP/α_{1b}-GFP + myc-CCR5). The results are the mean ± S.E. from three independent experiments. **, paired Student's *t* test, $p < 0.001$ compared with α_{1b}-CFP/α_{1b}-GFP.

calculated over 28 independent experiments was 0.09 ± 0.02, the average value of the GFP:CFP ratio being 1.25 ± 0.27. As expected, increasing the acceptor:donor ratio resulted in an increased energy transfer efficiency (results not shown). However, all the FRET measurements considered in this study were from experiments in which the GFP:CFP ratio was close to 1.

Hetero-oligomerization of the α_{1b}-AR and Its Selectivity—To test whether the α_{1b}-AR could form hetero-oligomers with

other GPCRs, we selected a number of receptors belonging to the rhodopsin-like sub-family: the α_{1a}-AR, the β_2-AR, the NK1 tachykinin receptor, and the CCR5 chemokine receptor. The CFP- or GFP-tagged receptor constructs were all inserted into the plasma membrane of HEK-293 cells as shown in Fig. 1.

FRET experiments in HEK-293 cells co-expressing the α_{1a}-CFP and α_{1a}-GFP constructs indicated that, like the α_{1b}-AR, the α_{1a}-AR subtype can form homo-oligomers (Fig. 3). In addi-
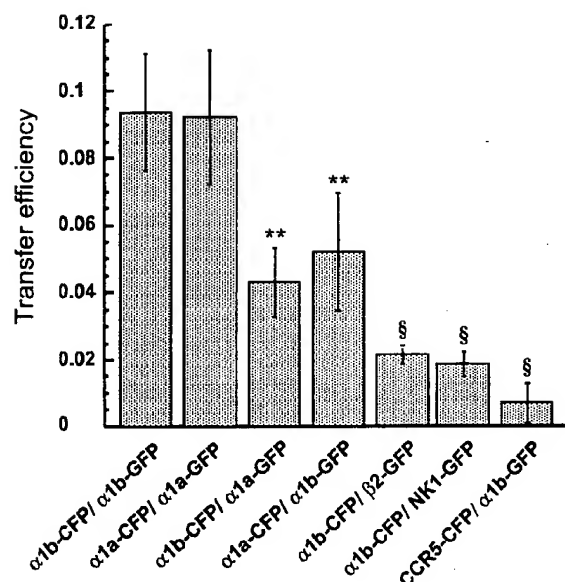
Fig. 3. **Homo- and hetero-oligomerization of the α_{1a} and α_{1b}-AR subtypes.** Energy transfer was measured in HEK-293 cells co-expressing different combinations of CFP- and GFP-tagged α_{1b}-AR, α_{1a}-AR, β_2-AR, tachykinin NK1, and chemokine CCR5 receptors. The results are the mean ± S.E. from 5 to 10 independent experiments. **, unpaired Student's t test, $p < 0.01$ compared with α_{1b}-CFP/α_{1b}-GFP; §, unpaired Student's t test, $p < 0.01$ compared with α_{1a}-CFP/α_{1b}-GFP.

tion, FRET experiments in cells expressing the α_{1b}-CFP/α_{1a}-GFP or α_{1a}-CFP/α_{1b}-GFP couples revealed that the α_{1a}- and α_{1b}-AR subtypes can form hetero-oligomers with each other as indicated by the value of the energy transfer efficiency of ~0.05 (Fig. 3). In contrast, in cells expressing the α_{1b}-CFP/β_2-GFP, α_{1b}-CFP/NK1-GFP, or CCR5-CFP/α_{1b}-GFP couples, a negligible FRET signal was detected. In agreement with these results, co-expression of the wild type CCR5 receptor with α_{1b}-CFP and α_{1b}-GFP was unable to decrease the FRET signal resulting from the homo-oligomerization of the α_{1b}-AR (Fig. 2C). These results suggest that the α_{1b}-AR can selectively form hetero-oligomers with the α_{1a}-AR subtype, but not with other GPCRs, like the/β_2-AR, NK1, and CCR5 receptors.

Co-immunoprecipitation Experiments—To validate the results from the FRET experiments, we aimed at investigating receptor oligomerization using the co-immunoprecipitation approach employed in a large number of studies to document oligomerization of GPCRs. The receptors were tagged as follows: the α_{1b}-AR with either HA or Myc at its C-tail; the α_{1a}-AR was tagged with HA at its C-tail; the NK1 receptor with Myc at its C-tail; and the CCR5 receptor with Myc at its N terminus. As mentioned above, the HA- or Myc-tagged α_1-AR subtypes displayed functional properties similar to those of the non-tagged receptors (Table I).

In the experiment shown in Fig. 4, differently tagged receptors were expressed either alone or in combination in HEK-293 cells, and a polyclonal anti-HA antibody was used to immunoprecipitate the receptors. Monoclonal anti-Myc (Fig. 4A) or anti-HA (Fig. 4B) antibodies was used for the immunoblot of the immunoprecipitated samples. As expected, the anti-Myc antibodies did not reveal any bands on Western blots of the immunoprecipitates from cells expressing the individual receptors α_{1b}-AR, α_{1b}-HA, α_{1b}-myc, α_{1a}-HA, or myc-CCR5 (Fig. 4A, *lanes 1–5*). In contrast, a predominant band of ~67 kDa corresponding to the α_{1b}-myc could be detected in the immunoprecipitate from cells co-expressing either the α_{1b}-HA/α_{1b}-myc or the α_{1a}-HA/α_{1b}-myc couples (Fig. 4A, *lanes 7 and 8*). The migration pattern of the α_{1b}-myc (one main band of ~67 kDa and
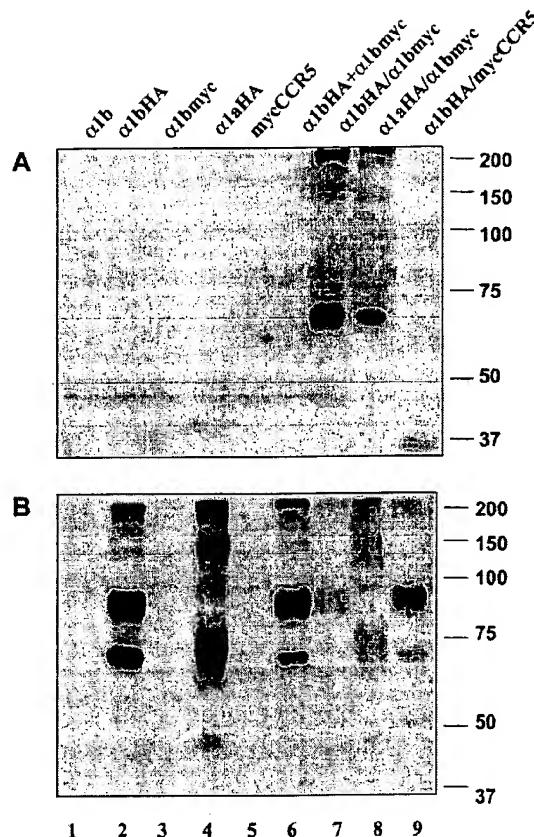

1 2 3 4 5 6 7 8 9

Fig. 4. **Co-immunoprecipitation of HA- and Myc-tagged receptor constructs.** The receptors were immunoprecipitated using anti-HA polyclonal antibodies from HEK-293 cells individually expressing the α_{1b}-AR (*lane 1*), different tagged receptors (*lanes 2–5*, α_{1b}-HA, α_{1b}-myc, α_{1a}-HA, and myc-CCR5, respectively), from a mixture of cells individually expressing the α_{1b}-HA and α_{1b}-myc (*lane 6*), or from cells co-expressing different tagged receptors (*lanes 7–9*, α_{1b}-HA/α_{1b}-myc, α_{1a}-HA/α_{1b}-myc, and α_{1b}-HA/myc-CCR5, respectively). The immunoblots were revealed using monoclonal anti-Myc (A) or anti-HA (B) antibodies. The blots are representative of five independent experiments.

a much fainter species of ~75 kDa) was different from that described previously for the wild type α_{1b}-AR (one fully glycosylated band at ~95 kDa and one core-glycosylated band at ~67 kDa (22)). This suggests that tagging the C-tail of the receptor with a Myc epitope modifies the maturation process of the receptor. Similar bands were observed also in membranes from cells expressing the α_{1b}-myc (results not shown).

To detect the presence of the various HA-tagged receptors in the immunoprecipitates, Western blots were also revealed using monoclonal anti-HA antibodies (Fig. 4B). Specific receptor bands were detected in all the immunoprecipitates from cells expressing different HA-tagged receptors. The immunoprecipitated α_{1b}-HA (Fig. 4B, *lanes 2, 6, 7,* and *9*) displayed two main bands at ~67 and ~95 kDa corresponding to those identified previously as the core-glycosylated and fully glycosylated forms of the non-tagged receptor, respectively (22). In contrast, the immunoprecipitated α_{1a}-HA displayed two predominant bands of ~70 and ~150 kDa and a much fainter species of ~100 kDa (Fig. 4B, *lanes 4* and *8*). Because the glycosylation pattern of the wild type α_{1a}-AR has not been fully characterized, the migration pattern of the HA-tagged receptor cannot be interpreted.

Altogether, these findings indicate that the α_{1b}-myc can be co-immunoprecipitated with the α_{1b}-HA as well as with the α_{1a}-HA co-expressed in the same cells. No α_{1b}-HA-α_{1b}-myc complex was observed when a mixture of cells individually

expressing the tagged receptors was subjected to the same immunoprecipitation procedure (Fig. 4A, lane 6). These results seem to support the conclusions from the FRET experiments indicating that the α_{1b}-AR could form homo-oligomers as well as hetero-oligomers with the α_{1a}-AR. However, in cells co-expressing the two receptors immunoprecipitation of the α_{1b}-HA resulted in the co-immunoprecipitation of a small portion of the Myc-tagged CCR5 chemokine receptor which was detected as an ~37-kDa band (Fig. 4A, lane 9). Similar results were also obtained with the NK1-myc which could be co-immunoprecipitated with the α_{1b}-HA (data not shown). These findings are somehow in conflict with those from the FRET experiments that demonstrated a negligible interaction of the α_{1b}-AR with the CCR5 and NK1 receptors.

Structural Determinants of the α_{1b}-AR Potentially Involved in Homo-oligomerization—So far, the mechanism by which GPCRs form oligomers has been poorly elucidated at a molecular level. Several hypotheses have been suggested including transmembrane domain swap (9), disulfide links between N-terminal domains (26), or dimerization motifs within the transmembrane helices (14). Among the structural determinants of the α_{1b}-AR potentially involved in receptor oligomerization, we initially investigated the role of its bulky C terminus, of the glycophorin dimerization motifs G*XXX*G in helix II and VI, as well as that of the *N*-linked glycosylation occurring at the N terminus.

To investigate whether the C terminus played a role in receptor oligomerization, we used a truncated α_{1b}-AR mutant, Thr^{369}, lacking the last 146 amino acids. The fluorescent constructs Thr^{369}-CFP and Thr^{369}-GFP were transiently co-expressed in HEK-293 cells. Comparison of the fluorescence spectra from cells expressing the Thr^{369}-CFP or Thr^{369}-GFP individually with those from cells co-expressing the two constructs indicated that the truncated mutant was able to form oligomers. This indicates that the integrity of the C-tail is not required for α_{1b}-AR homo-oligomerization. Moreover, the FRET efficiency measured between Thr^{369}-CFP and Thr^{369}-GFP was 44% higher than that between the α_{1b}-CFP and α_{1b}-GFP (Fig. 5). This could be explained by the fact that, in the absence of the flexible C terminus, the average donor-acceptor distance is decreased.

For glycophorin A, a protein with a single transmembrane segment forming SDS-resistant dimers, a specific motif G*XXX*G situated in the helical transmembrane domain is involved in its dimerization. The glycophorin motif G*XXX*G (27) can also be found in some GPCRs. In particular, it was reported previously (14) that in the β_2-AR replacing the glycines with alanines in the glycophorin motif in helix 6 destabilized receptor oligomerization. In the α_{1b}-AR, two G*XXX*G motifs can be found in helices II and VI. To explore their role in receptor oligomerization, we constructed two mutants, G53L and G301L, in which Gly^{53} and Gly^{301} belonging to glycophorin motifs in helices II and VI, respectively, were mutated into leucines. For each mutant, the CFP- and GFP-tagged constructs were co-expressed in HEK-293 cells; the analysis of the emission spectra indicated that FRET occurred with an efficiency comparable with that between α_{1b}-CFP and α_{1b}-GFP (Fig. 5). Altogether these findings suggest that the glycophorin motifs identified in the α_{1b}-AR are not involved in receptor homo-oligomerization.

To test if glycosylation of the receptor might contribute to α_{1b}-AR oligomerization, we measured FRET efficiency between CFP- and GFP-tagged constructs of the receptor mutant, N4, carrying the mutation of the four glycosylation sites present in the N terminus of the receptor. As described previously, the N4 mutant lacked *N*-linked glycosylation but retained its binding
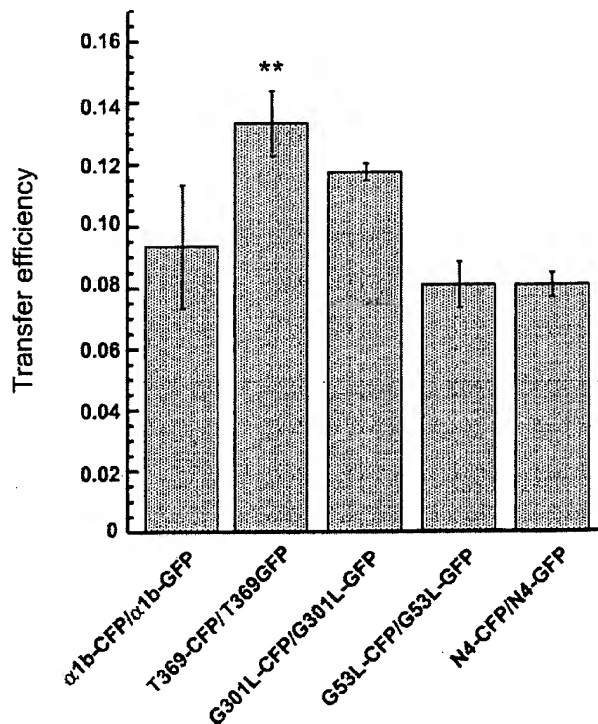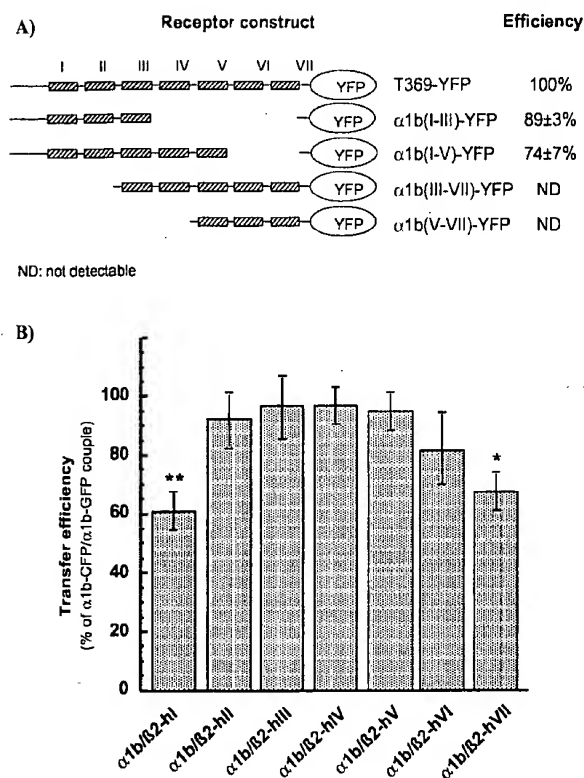

FIG. 5. **FRET measurements in cells expressing the α_{1b}-AR mutants carrying a truncation of the C-tail or mutations of the glycophorin motifs or glycosylation sites.** Energy transfer was measured in HEK-293 cells co-expressing the CFP- and GFP-tagged forms of the α_{1b}-AR or of the Thr^{369}, G53L, G301L, and N4 mutants. The results are the mean ± S.E. of three to nine independent experiments. **, unpaired Student's *t* test, $p < 0.01$ compared with α_{1b}-CFP/α_{1b}-GFP.

and signaling properties (22). The FRET signal measured between the N4-CFP and N4-GFP was comparable with that between α_{1b}-CFP and α_{1b}-GFP (Fig. 5). These results seem to exclude a role of the *N*-linked glycosylation occurring at the N terminus of the α_{1b}-AR in receptor homo-oligomerization.

Because of these negative results, we investigated whether distinct transmembrane helices were specifically involved in receptor oligomerization. The hypothesis that transmembrane helices are involved in GPCR oligomerization has become increasingly accepted even if it has been demonstrated only for few receptors.

As a first approach, we generated receptor fragments of the α_{1b}-AR lacking different transmembrane helices and tested their ability to oligomerize with the receptor. The receptor fragments were constructed by progressively deleting groups of consecutive helices from the N or the C terminus of the receptor. In all receptor fragments the N terminus was preserved on the extracellular side and the fluorescent tag intracellularly. To improve the sensitivity of the FRET assay, in each fragment the YFP was fused in proximity of the C terminus of its last helix. In addition, to keep the fluorophores in greater proximity, FRET experiments were performed using the truncated receptors Thr^{369}-CFP and Thr^{369}-YFP lacking the C-tail. The energy transfer efficiency measured between the Thr^{369}-CFP and Thr^{369}-YFP receptors was 0.21 ± 0.02 ($n = 5$), which is significantly higher than that measured for Thr^{369} tagged with the CFP/GFP fluorophore couple (results not shown).

Confocal microscopy indicated that the receptor fragments fused to YFP were expressed at a similar level, and their fluorescence was uniformly distributed in the cytosol and around the nucleus thus suggesting its localization in the en-

A)

B)

FIG. 6. **FRET in cells expressing chimeric α_{1b}/β_2 or receptor fragments.** *A*, FRET efficiency was measured in HEK-293 cells co-expressing the truncated α_{1b}-AR mutant, Thr^{369}-CFP, and different α_{1b}-AR fragments fused to YFP. Results are mean ± S.E. of three independent experiments and are expressed as % of the FRET efficiency obtained with Thr^{369}-CFP/T39-YFP couple. *ND*, no FRET signal could be detected. *B*, energy transfer was measured in HEK-293 cells co-expressing the α_{1b}-CFP and different α_{1b}/β_2-AR chimeras fused to GFP. Results are mean ± S.E. of four to six independent experiments and are expressed as % of the FRET efficiency obtained with the α_{1b}-CFP/α_{1b}-GFP couple. *, unpaired Student's *t* test. $p < 0.05$ compared with α_{1b}-CFP/α_{1b}-GFP. **, unpaired Student's *t* test, $p < 0.01$ compared with α_{1b}-CFP/α_{1b}-GFP.

doplasmic reticulum (ER) (results not shown).

As shown in Fig. 6*A*, co-expression of the Thr^{369}-CFP with the receptor fragments α1b(I–III) or α1b(I–V) including helices I–III and I–V, respectively, resulted in a strong FRET signal comparable with that obtained with the whole truncated receptor. In contrast, co-expression with the receptor fragments α1b(III–VII) or α1b(V–VII), lacking helices I and II, did not result in any FRET signal. These results strongly suggest that the structural determinants playing a major role in the homo-oligomerization of the α_{1b}-AR are localized within helices I and/or II. In addition, given the ER localization of the receptor fragments, our results also indicate that FRET can efficiently occur in the ER. Altogether these findings are strong agreement with those recently obtained on the Ste2 pheromone receptor homo-oligomers (28) or on the oxytocine/vasopressin hetero-oligomers (29).

To investigate further the role of the transmembrane helices in α_{1b}-AR oligomerization, we took advantage of the low energy transfer efficiency measured between fluorescent α_{1b}- and β_2-AR (Fig. 3), and we selectively replaced each single helix of the α_{1b}-GFP-receptor with the corresponding helix of the β_2-AR. We decided to construct α_{1b}-AR chimeras using portions of the β_2-AR instead of those from less closely related receptors to better preserve receptor function. Our hypothesis was that, if one helix was prominently involved in homo-oligomerization, its replacement would result in a decreased FRET signal. Co-
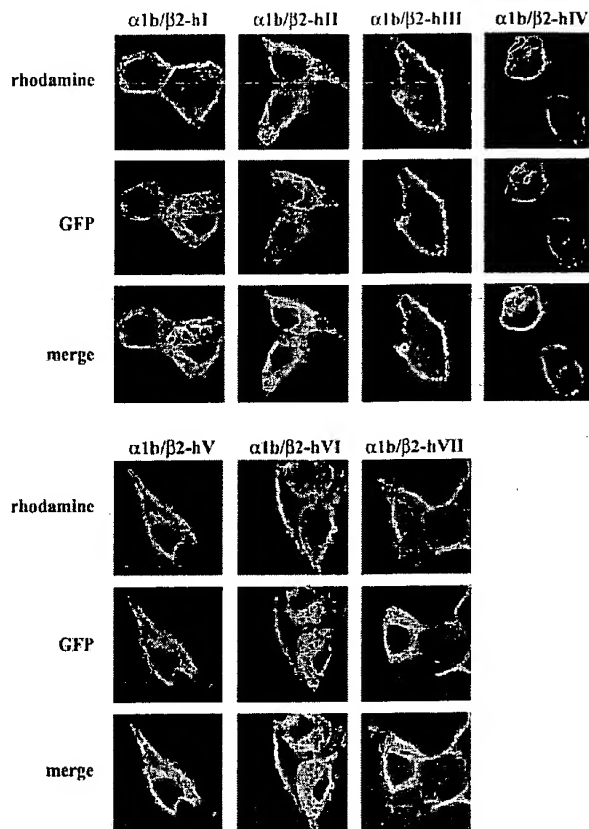
FIG. 7. **Co-expression of the α_{1b}-AR and chimeric α_{1b}/β_2 receptors.** Confocal images were taken on fixed HEK-293 cells expressing α_{1b}-HA and different α_{1b}/β_2 chimeras fused to GFP. Anti-HA polyclonal antibodies, followed by anti-rabbit antibodies labeled with rhodamine, were used to detect the α_{1b}-HA receptor. Images were taken after excitation at 488 nm for GFP or 543 nm for rhodamine. *Merge* represents the superimposition of the GFP and rhodamine images.

expression of the β_2-AR with the α_{1b}-CFP and α_{1b}-GFP receptors did not decrease the energy transfer thus indicating that the β_2-AR did not compete for the homo-oligomerization of the α_{1b}-AR (results not shown).

Confocal microscopy indicated that all the chimeric receptors were expressed at similar levels (Fig. 7). The α_{1b}/β_2-hIII and α_{1b}/β_2-hIV were mainly expressed at the plasma membrane, whereas the α_{1b}/β_2-hI, α_{1b}/β_2-hII, α_{1b}/β_2-hVI, α_{1b}/β_2-hV, and α_{1b}/β_2-hVII were localized in the ER with a faint plasma membrane labeling.

The chimeric receptors α_{1b}/β_2-hIII and α_{1b}/β_2-hIV displayed a normal [^{125}I]HEAT binding, but markedly decreased epinephrine-induced IP response (Table II). This suggests that replacement of helices III or IV, despite not perturbing the expression of the receptor at the plasma membrane, markedly decreases its ability to be activated. The α_{1b}/β_2-hV chimera displayed normal expression, detected by [^{125}I]HEAT binding, as well as normal agonist-induced IP response despite a large decrease of affinity for epinephrine. [^{125}I]HEAT binding as well as receptor signaling were not measurable at the chimeric receptors α_{1b}/β_2-hII and α_{1b}/β_2-hVII. Only a small amount of [^{125}I]HEAT and agonist-induced response could be detected at chimeric receptors α_{1b}/β_2-hI and α_{1b}/β_2-hVI. Altogether these findings suggest that replacement of helices I, II, VI, or VII had the most profound effect on receptor expression at the plasma membrane and/or on its ligand binding properties.

FRET was measured in cells co-expressing the wild type α_{1b}-CFP and each of the six α_{1b}/β_2 chimeric receptors fused to

TABLE II
Pharmacological properties of the $\alpha 1b/\beta 2$ chimeras

[^{125}I]HEAT binding was measured on membranes prepared from HEK-293 cells expressing the $\alpha 1b$-AR and the $\alpha 1b/\beta 2$ chimeras tagged with GFP. Expression was measured using 250 pM [^{125}I]HEAT on membranes from 1 well of a 6-well dish (200 μg of proteins/well). The inositol phosphate (IP) accumulation in the presence of 10^{-4} M epinephrine (Epi-stimulated) is expressed as % of the levels measured in mock-transfected cells. Results are the mean $\pm$ S.E. of three independent experiments performed in triplicate. IC$_{50}$ values are representative of two independent experiments. ND, not detectable.

Receptor	Expression	Epi-stimulated IP	IC$_{50}$ Epi
	fmol/well	*%*	*μM*
$\alpha 1b$-AR	614 $\pm$ 106	1138 $\pm$ 211	5.6 $\pm$ 0.4
$\alpha 1b/\beta 2$-hI	63 $\pm$ 17	201 $\pm$ 20	
$\alpha 1b/\beta 2$-hII	ND	102 $\pm$ 3	
$\alpha 1b/\beta 2$-hIII	545 $\pm$ 60	111 $\pm$ 30	140
$\alpha 1b/\beta 2$-hIV	685 $\pm$ 240	104 $\pm$ 4	240
$\alpha 1b/\beta 2$-hV	650 $\pm$ 90	1308 $\pm$ 9	>1000
$\alpha 1b/\beta 2$-hVI	80 $\pm$ 3	499 $\pm$ 106	
$\alpha 1b/\beta 2$-hVII	ND	131 $\pm$ 15	

GFP. As shown in Fig. 6B, a FRET signal could be measured under each condition. In particular, the energy transfer efficiency in cells expressing the fluorescent α_{1b}/β_2-hII, α_{1b}/β_2-hIII, α_{1b}/β_2-hIV, α_{1b}/β_2-hV, and α_{1b}/β_2-hVI was similar to that of cells expressing the wild type α_{1b}-CFP/α_{1b}-GFP couple. In contrast, the FRET signals measured in cells expressing the fluorescent α_{1b}/β_2-hI and α_{1b}/β_2-hVII were 40 and 25% lower, respectively. This indicates that the integrity of helix I and, to a lesser extent, that of helix VII are required for α_{1b}-AR homo-oligomerization. The results obtained on the receptor fragments indicated that only those including helix I ($\alpha 1b$(I–III) or $\alpha 1b$(I–V)) could associate with the receptor. Therefore, we suggest that in the whole α_{1b}-AR helices I and VII, which are close to each other within the helical bundle, act in concert in favoring receptor homo-oligomerization, with helix I being the prominent interface. The symmetrical or asymmetrical nature of the inter-helical interactions involved in receptor oligomerization will require additional studies.

To support the results from the FRET experiments, we used confocal microscopy to investigate the localization of the chimeric receptors fused to GFP in cells co-expressing the wild type α_{1b}-HA. As shown in Fig. 7, the chimeric receptors that did not display a significant decrease of the FRET signal (α_{1b}/β_2-hII, α_{1b}/β_2-hIII, α_{1b}/β_2-hIV, α_{1b}/β_2-hV, and α_{1b}/β_2-hVI) co-localize with the wild type receptor as indicated by the overlapping of the green and red fluorescence both at the plasma membrane and in the cytosol (Fig. 7, *merge*). This supports the hypothesis that these chimeric receptors can oligomerize with the α_{1b}-AR. In contrast, in cells co-expressing the α_{1b}/β_2-hI and the wild type receptor, the green and red fluorescence did not overlap at all, thus suggesting that the receptors do not co-segregate within the same cellular localization. This supports the hypothesis that the ability of the α_{1b}/β_2-hI chimera to oligomerize is significantly reduced as indicated by the FRET results (Fig. 6). The α_{1b}/β_2-hVII chimera displayed also some co-localization with the α_{1b}-AR at the plasma membrane which was, however, less pronounced than for the α_{1b}/β_2-hIII and α_{1b}/β_2-hIV. This is consistent with the fact that the α_{1b}/β_2-hVII displays a small decrease in its ability to oligomerize as indicated by the FRET results (Fig. 6).

For those chimeric receptors that were mainly expressed at the plasma membrane (α_{1b}/β_2-hIII and α_{1b}/β_2-hIV), the co-localization with the wild type receptor could be clearly appreciated at the cell surface. For those found in the ER and, to a lesser extent, in the plasma membrane (α_{1b}/β_2-hII, α_{1b}/β_2-hV, and α_{1b}/β_2-hVI), the co-localization was evident at both locations suggesting that the wild type receptor was partially re-
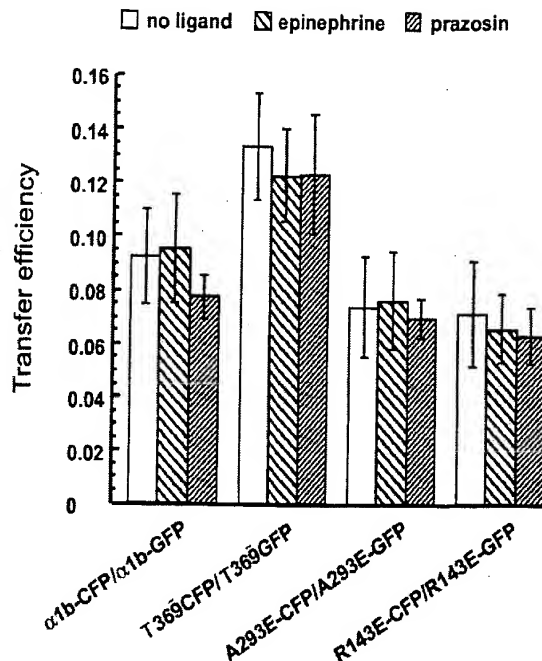
☐ no ligand ◣ epinephrine ▨ prazosin

FIG. 8. **Effect of ligands and activation on oligomerization of the α_{1b}-AR.** Energy transfer was measured in HEK-293 cells co-expressing the CFP- and GFP-tagged forms of the α_{1b}-AR or of the Thr^{369} (truncated), A293E (constitutively active), and R143E (signaling-deficient) mutants. Emission spectra were monitored before (no ligand) or after the incubation for 15 min with the agonist (10^{-4} M epinephrine) or the inverse agonist (10^{-6} M prazosin) at 37 °C. The results are the mean $\pm$ S.E. of five to nine independent experiments.

tained inside the cell when co-expressed with the chimeric receptors.

The Effect of α_{1b}-AR Activation on Homo-oligomerization— To investigate whether oligomerization was dependent on the activation state of the α_{1b}-AR, we followed two different approaches. In the first approach, we took advantage of two receptor mutants previously characterized in other studies: the R143E which is signaling-deficient (20) and the A293E which is constitutively active (21). These receptor mutants were fused to CFP and GFP, and FRET was measured in HEK-293 cells co-expressing the CFP- and GFP-tagged constructs of each receptor mutant. As shown in Fig. 8, both the R143E and A293E mutants proved able to form homo-oligomers, and the FRET efficiency was not significantly different from that measured for the wild type α_{1b}-AR homo-oligomers.

As a second approach, we tested whether receptor ligands could have an effect on receptor homo-oligomerization. Cells expressing different fluorescent receptor constructs were incubated for 15 min at 37 °C with the agonist epinephrine or the inverse agonist prazosin. As shown in Fig. 8, no significant ligand-induced effect on the energy transfer efficiency could be detected under our experimental conditions. Altogether these findings suggest that the α_{1b}-AR homo-oligomers are constitutively formed and independent from the activation state of the receptor as well as from ligand binding. Nevertheless, we cannot discredit the hypotheses that a putative ligand effect fell beyond the sensitivity range of our measurement or that the conditions under which the experiments were carried out were too distant from physiological parameters.

*Pharmacological Investigation of the Receptor Oligomers—*It has been reported previously (30–32) that co-expression of different GPCRs in cells can modify the binding properties of ligands resulting either in binding cooperativity or in a new pharmacological profile. Therefore, we compared the binding

properties of a number of ligands in membranes derived from cells expressing the α_{1a}- and α_{1b}-AR individually or in combination. In addition, the ligand binding curves on membranes from cells co-expressing the two receptor subtypes were compared with those measured on a 1:1 mixture of membranes from cells individually expressing the receptors. Competition binding curves using the non-selective radioligand [125I]HEAT were measured for the non-selective agonists epinephrine and norepinephrine, for the α_{1a}-selective agonists oxymetazoline and cirazoline, for the non-selective antagonist prazosin, as well as for the α_{1a}-selective antagonists 5-methylurapidil and phentolamine. The K_I values of the non-selective ligands were similar at the receptors expressed individually or in combination, whereas the α_{1a}-selective ligands displayed biphasic competition curves in membranes from cells co-expressing the α_{1a}- and α_{1b}-AR (results not shown). Similar competition curves were obtained on a 1:1 mixture of membranes derived from cells individually expressing the α_{1a}- and α_{1b}-AR (results not shown). In conclusion, the ligand binding curves did not detect any additional binding sites or change in the Hill coefficient that could be attributed to receptor oligomers. Two interpretations can be given for these results. One possibility is that α_1-AR hetero-oligomerization does not influence the pharmacological properties of the receptors within the oligomer. Another possibility is that the amount of receptor hetero-oligomers is too small to result in any detectable pharmacological change.

Internalization of the Receptor Oligomers—It has been reported previously that receptor oligomerization can play a role in the trafficking of GPCRs (17, 18, 33, 34). We therefore used confocal imaging to investigate the internalization properties of differently tagged α_1-AR subtypes, CCR5 and NK1 receptors expressed alone or in combination in HEK-293 cells. In particular, we made the hypothesis that only those receptors predicted to form oligomers based on the FRET experiments would mutually influence their internalization properties.

Confocal imaging of HEK-293 cells transfected with different DNAs using the calcium-phosphate method revealed that 30–50% of cells were routinely transfected and that receptors were co-localized in about 50% of the transfected cells. As shown in Fig. 9, exposure of cells expressing the α_{1b}-GFP to epinephrine for 1 h resulted in receptor internalization, as demonstrated by the marked increase in the intracellular green fluorescence. To explore the role of hetero-oligomerization on receptor endocytosis, the α_{1b}-GFP and the α_{1a}-HA were co-expressed in HEK-293 cells and exposed to 10^{-5} M oxymetazoline that can selectively activate the α_{1a}-AR but not the α_{1b}-AR subtype. As shown in Fig. 9, oxymetazoline was unable to induce the internalization of the α_{1b}-GFP, whereas it triggered the internalization of the α_{1a}-HA. Interestingly, in cells co-expressing the two receptors, oxymetazoline-induced internalization of the α_{1a}-HA drove the endocytosis of the α_{1b}-GFP as demonstrated by the co-localization of the green and red fluorescence within the cell (Fig. 9, *merge*).

The NK1-GFP expressed in HEK-293 cells could also undergo endocytosis in response to substance P, but not to epinephrine (Fig. 10). In cells co-expressing the NK1-GFP and α_{1b}-HA, exposure to epinephrine did not induce internalization of the NK1-GFP, and vice versa, treatment with substance P did not trigger the internalization of the α_{1b}-HA, as demonstrated by the clear segregation of the green and red fluorescent markers (Fig. 10, *merge*).

Similar results were obtained in cells co-expressing the α_{1b}-HA and myc-CCR5 (Fig. 11). In cells co-expressing the myc-CCR5 and α_{1b}-HA, exposure to epinephrine did not induce internalization of the myc-CCR5, and vice versa, treatment
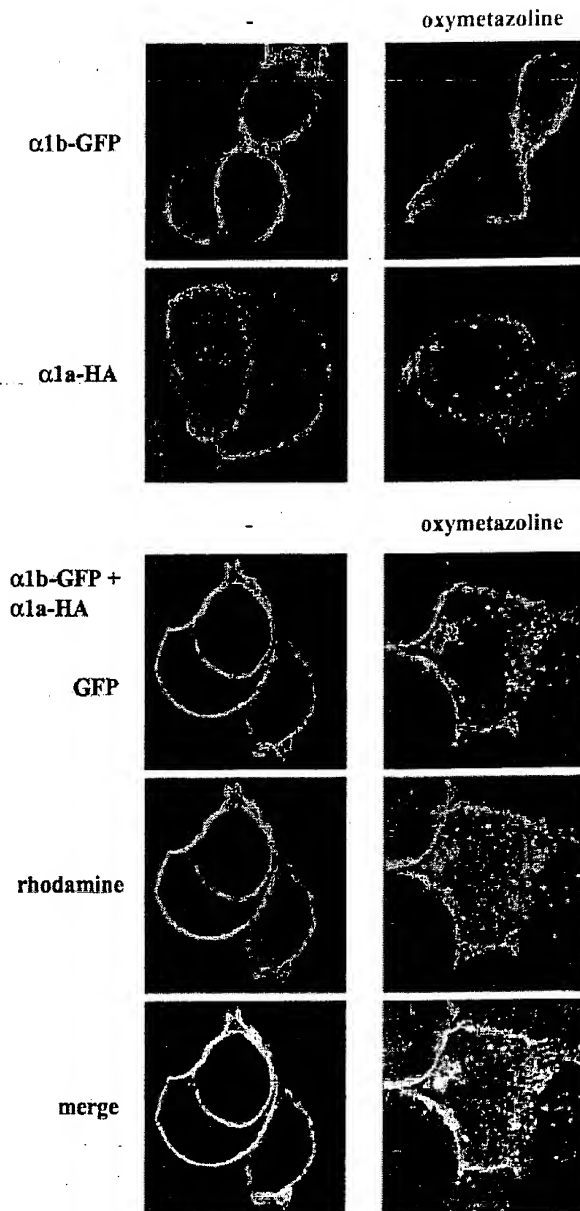
FIG. 9. **Co-internalization of the α_{1a}- and α_{1b}-AR subtypes.** Confocal images were taken on fixed HEK-293 cells expressing the α_{1b}-GFP and α_{1a}-HA individually or in combination (α_{1b}-GFP + α_{1a}-HA) and incubated for 1 h in the absence or presence of 10^{-5} M oxymetazoline. Anti-HA polyclonal antibodies, followed by anti-rabbit antibodies labeled with rhodamine, were used to detect the α_{1a}-HA receptor. Images were taken after excitation at 488 nm for GFP or 543 nm for rhodamine. *Merge* represents the superimposition of the GFP and rhodamine images.

with RANTES did not trigger the internalization of the α_{1b}-HA, as shown by the fact that the green and red fluorescent markers did not overlap (Fig. 11, *merge*).

Altogether these findings strongly support the hypothesis that co-internalization is related to receptor oligomerization, because only those receptors forming oligomers in FRET experiments, like the α_{1a}- and α_{1b}-AR subtypes, were able to co-internalize.

DISCUSSION

The present study provides evidence that both the α_{1a}- and α_{1b}-AR subtypes can form homo- as well as hetero-oligomers
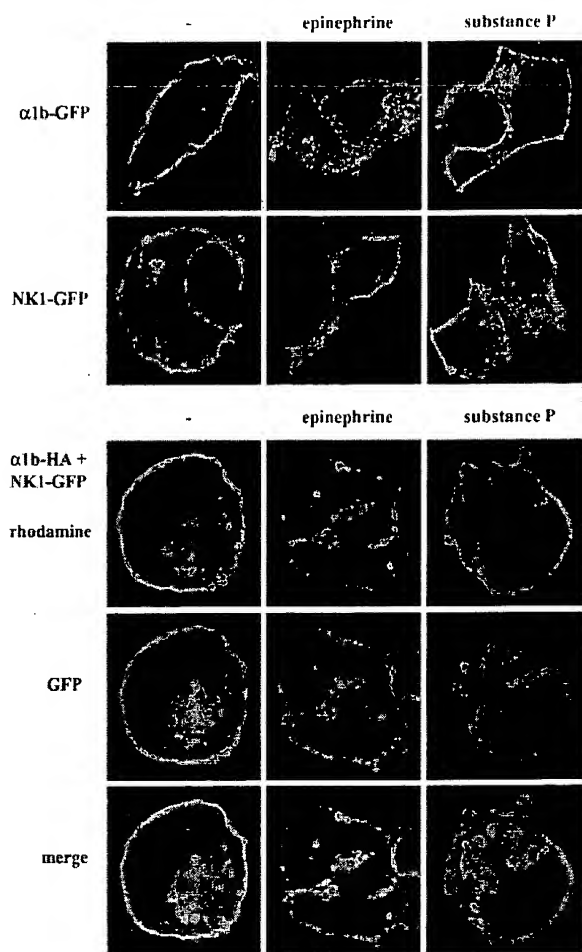
FIG. 10. **Lack of co-internalization of the α_{1b}-AR and NK1 receptor.** Confocal images were taken on fixed HEK-293 cells expressing the α_{1b}-GFP and NK1-GFP individually or co-expressing the α_{1b}-HA and NK1-GFP (α_{1b}-HA + NK1-GFP) incubated for 1 h in the absence or presence of 10^{-4} M epinephrine or 10^{-4} M substance P. Anti-HA polyclonal antibodies, followed by anti-rabbit antibodies labeled with rhodamine, were used to detect the α_{1b}-HA receptor. Images were taken after excitation at 488 nm for GFP or 543 nm for rhodamine. *Merge* represents the superimposition of the GFP and rhodamine images.
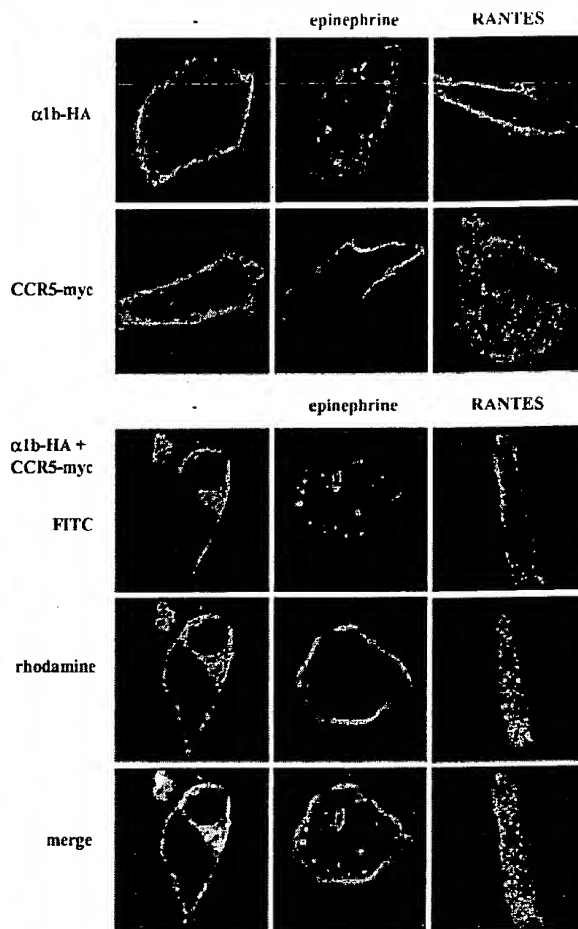
FIG. 11. **Lack of co-internalization of the α_{1b}-AR and CCR5 receptor.** Confocal images were taken on fixed HEK-293 cells expressing the α_{1b}-HA and myc-CCR5 individually or in combination (α_{1b}-HA + myc-CCR5) and incubated for 1 h in the absence or presence of 10^{-4} M epinephrine or 10^{-6} M RANTES. Anti-HA polyclonal and anti-Myc monoclonal antibodies followed by anti-rabbit antibodies labeled with FITC and anti-mouse antibodies labeled with rhodamine were used to detect the α_{1b}-HA and myc-CCR5, respectively. Images were taken after excitation at 488 nm for FITC or 543 nm for rhodamine. *Merge* represents the superimposition of the FITC and rhodamine images.

and that oligomerization correlates with the agonist-induced co-internalization of the receptors. In addition, it suggests a role of helices I and VII in homo-oligomerization of the α_{1b}-AR.

Oligomerization was mainly demonstrated monitoring FRET between receptors fused to donor CFP and acceptor GFP or YFP co-expressed in a transient expression system. As mentioned above, FRET only occurs when the average distance between the donor-acceptor pair falls below ~100 Å (10). However, whether a FRET between two fluorescent receptors involves intermolecular interactions among receptors *versus* their increased proximity within the cell membrane without direct contact cannot be unequivocally demonstrated by FRET. Another limitation of the energy transfer measurements is that, while detecting proximity between the fluorescent receptors, neither number of molecules per complex nor the fraction of the total receptor population existing in the oligomeric state can be assessed.

Despite these limits, our FRET show a selective pattern of receptor oligomerization. In fact, our results indicate that both the α_{1a}- and α_{1b}-AR form homo-oligomers with similar transfer efficiency of ~0.10 (Fig. 2). Hetero-oligomers between the α_{1a}- and α_{1b}-AR could also be observed, the FRET efficiency being in

this case of ~0.05. These results suggest that, when the α_1-AR subtypes are expressed at comparable levels, the trend to oligomerize is greater for the homo-oligomers than for the hetero-oligomers. In contrast, almost no FRET signal could be measured between the α_{1b}-AR and the β_2-AR, NK1 tachykinin, or the CCR5 chemokine receptors expressed at similar levels (Fig. 3). This strongly suggests that for the α_{1b}-AR the ability of forming hetero-oligomers with other GPCRs is related to the degree of sequence homology. This is also in agreement with the results from a recent study (33) showing that homo-oligomerization of the opioid receptors occurred more efficiently than their hetero-oligomerization with the β_2-AR.

An important observation of our study is that the results obtained from the co-immunoprecipitation experiments were not entirely consistent with those from the FRET measurements. In fact, when differently tagged receptors were co-expressed in HEK-293 cells the α_{1b}-AR could co-immunoprecipitate with the α_{1a}-AR as well as with a small amount of the CCR5 chemokine or NK1 tachykinin receptors (Fig. 4 and results not shown). Therefore, the conditions used in our experiments resulted in a certain promiscuity in the ability of the receptors to be co-immunoprecipitated. This suggests that the

results obtained using co-immunoprecipitation should be interpreted with some caution and, possibly, be confirmed using other independent approaches.

For some GPCRs the structural determinants involved in receptor oligomerization have been investigated. Whereas the C terminus is implicated in the $GABA_B$-R1/$GABA_B$-R2 receptor oligomerization (11), the glycophorin motif seems to be involved in the formation of β_2-AR homo-oligomers (14), and a role of the N terminus was reported for the oligomerization of the bradykinin and calcium receptors (36, 37). Our findings indicate that the α_{1b}-AR homo-oligomerization does not require the integrity of either the C-tail, the *N*-linked glycosylation sites in the N terminus, or the glycophorin motifs in helices II and VI (Fig. 5).

Recent crystallographic data from native membranes of mouse retina showed that rhodopsin, a prototypical GPCR, was arranged in the membrane as a paracrystalline lattice of dimers as structural units. The intradimeric contacts seem to involve helices IV and V, whereas helices I and II, as well as the cytoplasmic loop i3, might be involved in the formation of dimer rows (38). So far, based on mutagenesis and cross-linking experiments, helix VI for β-AR (14), helix IV for dopamine D_2 (39), or helices I and II for Ste2 pheromone receptor homo-oligomers (28) have been proposed to provide inter-monomeric contacts. A theoretical study on the opioid receptors based on the subtractive correlated mutation method predicted that in receptor homo-oligomerization the most likely interfaces are helices IV and V for the δ, helix V for the κ, and helix I for the μ receptors (40). Our findings provide the evidence that for the α_{1b}-AR helices I and VII act in concert favoring receptor homo-oligomerization with helix I representing a prominent interface. Altogether these results support the notion that GPCR oligomerization involves the participation of different transmembrane helices whose role might differ among receptors. In addition, our findings do not support a domain swapping oligomerization model because we were unable to rescue the functional properties of binding- and signaling-deficient α_{1b}-AR mutants co-expressed in the same cells (data not shown).

The ability of ligands to modulate GPCR oligomerization has been investigated by a large number of studies in which a wide range of possibilities can be found. In several cases agonists promoted association of receptors, *e.g.* the β_2-AR, the receptors for GnRH and TRH, as well as the chemokine CXCR4, the bradykinin B2 and SSR5 somatostatin receptors (16, 34, 41–45). However, in an equally large number of cases, oligomers appear to be constitutive, *e.g.* for the somatostatin receptors the m3 muscarinic receptor, and for the yeast pheromone Ste2 receptor (25, 46, 47), or to dissociate upon treatment with the agonist, like the δ-opioid or cholecystokinin receptor oligomers (48, 49). The basis for these discrepancies remains obscure and might, at least in part, be related to the different experimental approaches used to monitor receptor oligomerization. In our study, the α_{1b}-AR oligomers were found to be constitutive because neither the agonist epinephrine nor the inverse agonist prazosin had any effect on the FRET signal (Fig. 8). In addition, the oligomerization of the α_{1b}-AR did not seem to be related to its activation state because a constitutively active (A293E) as well as a signaling-deficient (R143E) mutant were equally able to associate with an energy transfer efficiency comparable with that of the wild type receptor (Fig. 8). Co-expression of the α_{1a}- and α_{1b}-AR did not result in any pharmacological changes that could be attributed to a novel receptor species resulting from receptor hetero-oligomerization (results not shown).

Despite the lack of ligand-induced regulation, our findings suggest that oligomerization of the α_1-AR subtypes might have functional implications in receptor endocytosis. In fact, we found that oligomerization of the α_1-AR subtypes correlated with their ability to co-internalize upon exposure to the agonist. Although the α_{1b}-AR could co-internalize with the α_{1a}-AR subtype (Fig. 9), it did not co-internalize with the NK1 tachykinin or CCR5 chemokine receptors (Figs. 10 and 11). Therefore, only the α_{1a}- and α_{1b}-AR subtypes, which could form hetero-oligomers, were able to co-internalize. The ability of the α_{1a}- and α_{1b}-AR subtypes to co-internalize might have physiological consequences on receptor regulation. The two receptors have an overlapping distribution in several tissues (*e.g.* heart, brain, prostate, etc.). One can expect that hetero-oligomerization might provide yet another means to fine-tune the responses mediated by the α_{1a}- and α_{1b}-AR subtypes like, for example, coordinating their internalization properties.

The literature on GPCR hetero-oligomerization harbors several examples of modified trafficking of one receptor upon association with another. For example, the rate of internalization of the β_2-AR (17) was markedly decreased when co-expressed with the κ-opioid receptor that does not undergo agonist-induced internalization. In contrast, the internalization of the δ-opioid receptor could trigger the co-internalization of the β_2-AR (17). As a consequence of its co-expression with mGluR1, the trafficking of the calcium receptor became susceptible to modulation by Homer, a protein known to interact with glutamate mGluRs (34). In the same study, internalization of the calcium receptor in response to glutamate was demonstrated to occur (34). Inhibition of the internalization of the β_2-AR was observed upon co-expression with β1-AR, which by itself internalizes to a lesser extent (18). The μ-opioid receptor could be internalized by exposure to a sst_{2A}-selective ligand in cells co-expressing the two receptors (33).

These examples indicate that the receptor partners associated in putative oligomers can mutually influence their internalization properties. However, a causal relationship between receptor oligomerization and internalization properties cannot be easily drawn. Co-internalization of two GPCRs could result from the recruitment to the plasma membrane of proteins belonging to the endocytic machinery following the agonist-induced activation of one of the receptors. However, in our study the co-internalization was selective for the α_{1a}- and α_{1b}-AR subtypes, whereas the recruitment of the endocytic machinery at the plasma membrane could be expected to enhance the internalization also of other GPCRs like the NK1 and CCR5 receptors. Based on this observation, we propose that the co-internalization of the α_{1a}- and α_{1b}-AR subtypes is directly related either to the co-segregation of the receptors in membrane micro-domains or to their intermolecular interaction.

An important issue concerning GPCR oligomerization is whether this phenomenon is due to the high levels of receptor expression in transient systems that might lead to receptor aggregation in the membrane. So far, the vast majority of the studies reporting oligomerization of GPCRs have been performed in such transient expression systems because of the free choice and convenient labeling of the target receptors. A recent study using bioluminescence resonance energy transfer reported that the number of β_2-AR oligomers could be consistently measured throughout a wide range of receptor expression levels (50). Because of the low sensitivity of the FRET measurements, in our study the expression of the fluorescent receptors could not be decreased below 1–2 pmol/mg of proteins. However, even if high levels of receptor expression might favor protein aggregation, the selectivity of the FRET signals observed for the α_1-AR subtypes strongly suggest that the energy transfer signals measured were not a mere consequence of receptor overexpression.

The results of our study as well as those from others (28, 29)

clearly indicate that receptor oligomerization can occur at the plasma membrane as well as in the ER. In fact, some of our findings suggest that α_1-AR oligomers exist at the plasma membrane, where epinephrine is acting to trigger receptor endocytosis, and that they do not dissociate during this process. However, given the ER localization of the receptor fragments and of some α_{1b}/β_2 chimeric receptors, their association with the α_{1b}-AR must occur at large extent in the ER. Altogether, these findings support the notion that oligomerization of the GPCRs is part of their maturation process playing a role in their export from the ER.

In conclusion, despite the growing number of studies on GPCR oligomerization, a number of aspects remain to be elucidated. In particular, the molecular mechanisms underlying GPCR oligomerization (*e.g.* intermolecular interaction *versus* co-segregation of receptors in microdomains; structural determinants of the receptor involved; number of receptor molecules per oligomer) cannot be unequivocally established. It is possible that, despite some common features, the oligomerization mechanisms might differ among GPCRs thus increasing the complexity of receptor signaling and regulation. Future studies should aim at investigating the role of receptor oligomerization in physiological systems as well as at further unraveling its molecular basis.

REFERENCES

1. Ghanouni, P., Gryczynski, Z., Steenhuis, J. J., Lee, T. W., Farrens, D. L., Lakowicz, J. R., and Kobilka, B. K. (2001) *J. Biol. Chem.* **276,** 24433–24436
2. Watson, C., Chen, G., Irving, P., Way, J., Chen, W. J., and Kenakin, T. (2000) *Mol. Pharmacol.* **58,** 1230–1238
3. Hur, E. M., and Kim, K. T. (2002) *Cell. Signal.* **14,** 397–405
4. Selbie, L. A., and Hill, S. J. (1998) *Trends Pharmacol. Sci.* **19,** 87–93
5. Angers, S., Salahpour, A., and Bouvier, M. (2002) *Annu. Rev. Pharmacol. Toxicol.* **42,** 409–435
6. Devi, L. A. (2001) *Trends Pharmacol. Sci.* **22,** 532–537
7. Gomes, I., Jordan, B. A., Gupta, A., Rios, C., Trapaidze, N., and Devi, L. A (2001) *J. Mol. Med.* **79,** 226–242
8. Maggio, R., Barbier, P., Colelli, A., Salvadori, F., Demontis, G., and Corsini, G. U. (1999) *J. Pharmacol. Exp. Ther.* **291,** 251–257
9. Gouldson, P. R., Higgs, C., Smith, R. E., Dean, M. K., Gkoutos, G. V., and Reynolds, C. A. (2000) *Neuropsychopharmacology* **23,** S60–S77
10. Pollok, B. A., and Heim, R. (1999) *Trends Cell Biol.* **9,** 57–60
11. Margeta-Mitrovic, M., Jan, Y. N., and Jan, L. Y. (2000) *Neuron* **27,** 97–106
12. Ciruela, F., Escriche, M., Burgueno, J., Angulo, E., Casado, V., Soloviev, M. M., Canela, E. I., Mallol, J., Chan, W. Y., Lluis, C., McIlhinney, R. A., and Franco, R. (2001) *J. Biol. Chem.* **276,** 18345–18351
13. AbdAlla, S., Lother, H., el Massiery, A., and Quitterer, U. (2001) *Nat. Med.* **7,** 1003–1009
14. Hebert, T. E., Moffett, S., Morello, J. P., Loisel, T. P., Bichet, D. G., Barret, C., and Bouvier, M. (1996) *J. Biol. Chem.* **271,** 16384–16392
15. Hebert, T. E., Loisel, T. P., Adam, L., Ethier, N., Onge, S. S., and Bouvier, M.
(1998) *Biochem. J.* **330,** 287–293
16. Angers, S., Salahpour, A., Joly, E., Hilairet, S., Chelsky, D., Dennis, M., and Bouvier, M. (2000) *Proc. Natl. Acad. Sci. U. S. A.* **97,** 3684–3689
17. Jordan, B. A., Trapaidze, N., Gomes, I., Nivarthi, R., and Devi, L. A. (2001) *Proc. Natl. Acad. Sci. U. S. A.* **98,** 343–348
18. Lavoie, C., Mercier, J. F., Salahpour, A., Umapathy, D., Breit, A., Villeneuve, L. R., Zhu, W. Z., Xiao, R. P., Lakatta, E. G., Bouvier, M., and Hebert, T. E. (2002) *J. Biol. Chem.* **277,** 35402–35410
19. Cotecchia, S., Ostrowski, J., Kjelsberg, M. A., Caron, M. G., and Lefkowitz, R. J. (1992) *J. Biol. Chem.* **267,** 1633–1639
20. Scheer, A., Costa, T., Fanelli, F., De Benedetti, P. G., Mhaouty-Kodja, S., Abuin, L., Nenniger-Tosato, M., and Cotecchia, S. (2000) *Mol. Pharmacol.* **57,** 219–231
21. Mhaouty-Kodja, S., Barak, L. S., Scheer, A., Abuin, L., Diviani, D., Caron, M. G., and Cotecchia, S. (1999) *Mol. Pharmacol.* **55,** 339–347
22. Bjorklof, K., Lundstrom, K., Abuin, L., Greasley, P. J., and Cotecchia, S. (2002) *Biochemistry* **41,** 4281–4291
23. Schwinn, D. A., Johnston, G. I., Page, S. O., Mosley, M. J., Wilson, K. H., Worman, N. P., Campbell, S., Fidock, M. D., Furness, L. M., and Parry-Smith, D. J. (1995) *J. Pharmacol. Exp. Ther.* **272,** 134–142
24. Diviani, D., Lattion, A. L., and Cotecchia, S. (1997) *J. Biol. Chem.* **272,** 28712–28719
25. Overton, M. C., and Blumer, K. J. (2000) *Curr. Biol.* **10,** 341–344
26. Ray, K., Hauschild, B. C., Steinbach, P. J., Goldsmith, P. K., Hauache, O., and Spiegel, A. M. (1999) *J. Biol. Chem.* **274,** 27642–27650
27. Russ, W. P., and Engelman, D. M. (2000) *J. Mol. Biol.* **296,** 911–919
28. Overton, M. C., and Blumer, K. J. (2002) *J. Biol. Chem.* **277,** 41463–41472
29. Terrillon, S., Durroux, T., Mouillac, B., Breit, A., Ayoub, M. A., Taulan, M., Jockers, R., Barberis, C., and Bouvier, M. (2003) *Mol. Endocrinol.* **17,** 677–691
30. Yoshioka, K., Saitoh, O., and Nakata, H. (2001) *Proc. Natl. Acad. Sci. U. S. A.* **98,** 7617–7622
31. Rocheville, M., Lange, D. C., Kumar, U., Patel, S. C., Patel, R. C., and Patel, Y. C. (2000) *Science* **288,** 154–157
32. Jordan, B. A., and Devi, L. A. (1999) *Nature* **399,** 697–700
33. Pfeiffer, M., Koch, T., Schroder, H., Laugsch, M., Hollt, V., and Schulz, S. (2002) *J. Biol. Chem.* **277,** 19762–19772
34. Gama, L., Wilt, S. G., and Breitwieser, G. E. (2001) *J. Biol. Chem.* **276,** 39053–39059
35. McVey, M., Ramsay, D., Kellett, E., Rees, S., Wilson, S., Pope, A. J., and Milligan, G. (2001) *J. Biol. Chem.* **276,** 14092–14099
36. AbdAlla, S., Zaki, E., Lother, H., and Quitterer, U. (1999) *J. Biol. Chem.* **274,** 26079–26084
37. Pace, A. J., Gama, L., and Breitwieser, G. E. (1999) *J. Biol. Chem.* **274,** 11629–11634
38. Liang, Y., Fotiadis, D., Filipek, S., Saperstein, D. A., Palczewski, K., and Engel, A. (2003) *J. Biol. Chem.* **278,** 21655–21662
39. Guo, W., Shi, L., and Javitch, J. A. (2003) *J. Biol. Chem.* **278,** 4385–4388
40. Filizola, M., and Weinstein, H. (2002) *Biopolymers* **66,** 317–325
41. Angers, S., Salahpour, A., and Bouvier, M. (2001) *Life Sci.* **68,** 2243–2250
42. Cornea, A., Janovick, J. A., Maya-Nunez, G., and Conn, P. M. (2001) *J. Biol. Chem.* **276,** 2153–2158
43. Kroeger, K. M., Hanyaloglu, A. C., Seeber, R. M., Miles, L. E., and Eidne, K. A. (2001) *J. Biol. Chem.* **276,** 12736–12743
44. Vila-Coro, A. J., Rodriguez-Frade, J. M., Martin De Ana, A., Moreno-Ortiz, M. C., Martinez, A. C., and Mellado, M. (1999) *FASEB J.* **13,** 1699–1710
45. Patel, R. C., Kumar, U., Lamb, D. C., Eid, J. S., Rocheville, M., Grant, M., Rani, A., Hazlett, T., Patel, S. C., Gratton, E., and Patel, Y. C. (2002) *Proc. Natl. Acad. Sci. U. S. A.* **99,** 3294–3299
46. Rocheville, M., Lange, D. C., Kumar, U., Sasi, R., Patel, R. C., and Patel, Y. C. (2000) *J. Biol. Chem.* **275,** 7862–7869
47. Zeng, F. Y., and Wess, J. (1999) *J. Biol. Chem.* **274,** 19487–19497
48. Cvejic, S., and Devi, L. A. (1997) *J. Biol. Chem.* **272,** 26959–26964
49. Cheng, Z. J., and Miller, L. J. (2001) *J. Biol. Chem.* **276,** 48040–48047
50. Mercier, J. F., Salahpour, A., Angers, S., Breit, A., and Bouvier, M. (2002) *J. Biol. Chem.* **277,** 44925–44931